11th World Congress on Computational Mechanics (WCCM XI)
5th European Conference on Computational Mechanics (ECCM V)
6th European Conference on Computational Fluid Dynamics (ECFD VI)
E. Oñate, J. Oliver and A. Huerta (Eds)

COMPARISON OF THE LAMINAR-TURBULENT TRANSITION PREDICTION USING DIFFERENT METHODS WITH THE LAMINAR WING TEST RESULTS

SERGEY L. CHERNYSHEV, ALEXANDER I. IVANOV, ANDREY PH. KISELEV, VLADIMIR A. KUZMINSKY, DMITRY S. SBOEV, LEONID L. TEPERIN AND VALERY V. VOZHDAEV

Central Aerohydrodynamic Institute n.a. prof. N.E. Zhukovsky,
140180, Zhukovsky Moscow reg., Russia
e-mail: ivanov_a_i@list.ru,www.tsagi.ru

Key Words: boundary layer, transition, numerical methods, experiment.

Summary. *Basing on the comparison with the experimental data, the possibilities of application of different numerical methods for prediction of the laminar-turbulent transition and for investigation of the increased disturbances background effect on its characteristics are analyzed.*

1 INTRODUCTION

When designing the laminar airplane, particularly important are issues related to the free-stream turbulence effects and the extrapolation of the test data, obtained in industrial wind tunnels (WT), to flight conditions.

In connection with this, it is very important to verify different methods of the boundary layer stability and laminar-turbulent transition prediction by comparison of the CFD and experimental data. In particular, a special interest is shown in the definition of the calculated *N*-factor values, corresponding to the laminar-turbulent transition in test conditions at different initial turbulence levels.

Nowadays, the CFD-methods basing on the Reynolds-averaged Navier-Stokes equation solutions are widely used. These equations are closed using the semi-empirical turbulence models, with some of them being able to predict in principle also the laminar-turbulent transition characteristics. However, additional researches are demanded to define the operational limits of the existing turbulence models, to compare different models and to develop recommendations for their practical use.

The proposed study is the continuation of the researches completed in TsAGI in the framework of the TELFONA project [1] (6^{th} European FP). It is devoted to investigation of the possibilities to implement different calculation methods to the laminar-turbulent transition prediction and the influence of higher disturbance background level on its characteristics.

To analyze these effects, the detailed experimental studies [1-3] of transition zones on the straight and swept wing (leading edge sweep angle 35˚) with laminar profile LV6 were carried out in the low-turbulence wind tunnel. Both models had chord and span equal to 1m, possessing to obtain the Reynolds number of 5.4-5.5 million at flow velocity about 80 m/s.

The investigations of the incoming flow turbulence and acoustic disturbances effects on the laminar-turbulent transition were performed. To increase the incoming flow turbulence level special turbulizing grids were used. Both the time-averaged and unsteady flow components in the boundary layer were measured using the constant-temperature thermo-anemometer with a single hot-wire sensor. In the proposed report the results of such analyses for straight wing are presented.

2 EXPERIMENTAL EQUIPMENT AND WIND TUNNEL TESTING TECHNIQUE

2.1 Aerodynamic facility

Tests of LV6 laminar airfoil and swept wing models were targeted at the investigations of the influence of initial turbulence level of the flow and acoustic disturbances on laminar-turbulent transition. The experiments were conducted in TsAGI T-124 wind tunnel.

TsAGI T-124 subsonic wind tunnel (velocity range – U_0 = 2…100 m/s) is a closed-circuit compressor wind tunnel with test section dimensions of 1 m×1 m×4 m [4]. Wind tunnel T-124 is remarkable for sufficiently low initial turbulence level and low noise. These characteristics were achieved by means of applying high contraction ratio in the nozzle (17.6), high accuracy of maintaining the fan speed, using deturbulizing meshes in the settling chamber with the inner cell size of 0.7 mm, applying diffuser with a small opening angle, thorough finishing of the inner surfaces of the facility's channels and making of wood almost all basic elements of the wind tunnel with the exception of the test and fan sections. So, for the flow speed of less than 80 m/s the level of initial turbulence appears to be only 0.05%. It creates favorable conditions for researches of the boundary layers development leading, in the end, to the laminar-turbulent transition.

Since one of the goals of the given research is the investigation of the influence of initial flow turbulence level on the transition, in order to increase it two turbulizing grids were used, which were installed at the point of entry to the test section of the wind tunnel. Both grids have equal wire diameter of 1.5 mm but different cell sizes of 25 mm×25 mm (grid No.1) and 50 mm×50 mm (grid No.2). Both grids have considerably small cell sizes and, at the same time, acceptable level of the test section blockage.

The nature of the flow downstream of these grids was investigated in detail in the empty test section. The results of the average velocity measurements, both pneumometric and hot-wire ones, evidence that the non-homogeneity of the field in the form of the maximal deviation from the mean value is not larger than ±0.5% for the grid 25 mm×25 mm×1.5 mm and ±1.0% for the grid 50 mm×50 mm×1.5 mm. The root-mean-square (rms) values of the velocity fluctuation are equal to: longitudinal –0.59%, lateral –0.46% for the first grid (No.1). For the grid with larger cells (No.2) the corresponding values are 0.91% and 0.67%.

Additional measurements made using the single-wire gage of the constant-temperature anemometer (CTA) at the distance of 730 mm upstream from the model leading edge in the test section showed that levels of the rms fluctuation values for the longitudinal velocity component ε_u are equal to 1.26% behind the grid No.1 and 1.5% behind the grid No.2. These results as well as measurements over the model surface at X/C = 0.12 allow to make estimations for the turbulence level near the model leading edge, assuming that pulsations of the transversal velocity component are equal to the pulsations of the vertical one:

$$Tu = \sqrt{\frac{u_{rms}{}^2 + v_{rms}{}^2 + w_{rms}{}^2}{3U_0^2}},$$

where u_{rms}, v_{rms} and w_{rms} are rms pulsations of velocity components. So, for grid No.1 Tu = 0.61%, for grid No.2 Tu = 0.91% (for comparison, according to [4] for natural conditions Tu = 0.064%).

Acoustic disturbances were introduced into the flow by the dynamic loudspeaker with peak power of 50 W, installed in the test section window of the wind tunnel upstream of the model. The accuracy of the reproduction by the loudspeaker of the sound generator signal frequency was not worse than 0.1 Hz. During the measurement process, special attention was paid to the settling chamber temperature control, because this parameter strongly influences the characteristics of the acoustic waves introduced into the flow. The obtained values of sound pressure p_s appeared to be in the range 91-108 dB.

Both time-averaged and pulsating velocity components in the boundary layer were measured using CTA with the single-wire gage as a sensor. In order to move the hot-wire in the boundary layer near LV6 airfoil and swept wing models surface the compound coordinate mechanism was used, which includes the basic *XZ*-traverse gear and installed on it automated *Y*-traverse gear. The step size in the direction normal to model surface of the *Y* traverse gear was equal to 0.01mm.

2.2 Model description

LV6 airfoil model is a rectangular wing with the chord of 1000 mm and the span of 998 mm. The shape of the laminarized airfoil is close to symmetric one; its outline is shown in Figure1.

Figure 1: The LV6 airfoil

This airfoil was designed by DLR as part of the TELFONA Pathfinder Wing design activity. The model is placed in the closed test section of the wind tunnel T-124 from wall to wall at the equal distances from the floor and from the ceiling. Due to such position of the wing there is no tip vortices, the modeling of the flow over the “infinite span” wing is performed in the best way and the flow in the middle may be considered as two-dimensional one. The photographs of the LV6 airfoil model before and after installation in the test section of the T124 tunnel are shown in Figure2.

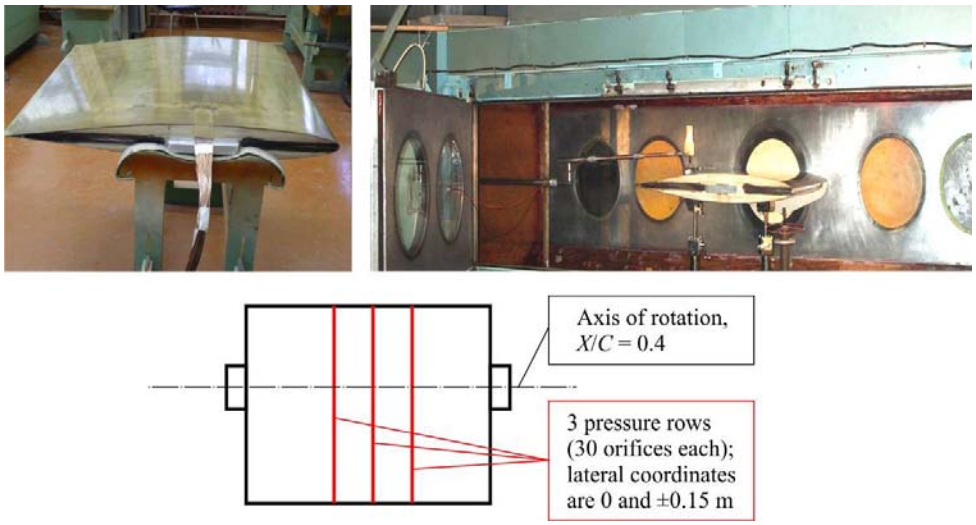

Figure 2: The LV6 airfoil model

The right photo shows also the *XZ*-traverse sting, the sting extender and *Y*-traverse gear.

The target of the tests was to explore the transition mechanisms for the 2D flow conditions. Before the main tests it was necessary to make sure that in the central part of the model there is an area where flow is independent of the lateral co-ordinate *Z*. For this purpose three rows of pressure taps were arranged (Figure 2). Also before the main measurements the *Y*-traverse influence on the averaged flow was investigated by means of the model pressure distributions comparison for two test conditions – with and without the *Y*-traverse gear. Data analyses showed that the traverse gear influence on the pressure distributions was rather small [2].

3 EXPERIMENTAL RESULTS

The tests were carried out at the flow velocity of 77.6 m/c, corresponding to the model chord Reynolds number $Re_\infty = 5.5\times10^6$ and the Mach number $M_\infty = 0.23$. All measurements were performed at the model angle of attack $\alpha = 0^o$ over the upper surface in the area of $X/C = 0.2\ldots0.7$ using the single-wire CTA gage.

Pressure distributions measured on both upper and lower model surfaces in three sections practically coincided with each other at the test conditions and the flow in the central zone might be considered as two-dimensional with good accuracy.

One of the most important experimental tasks of the work was to localize correctly the laminar-turbulent transition position.

When conducting the transition tests in natural conditions, there are certain difficulties connected with the a priori unknown character of the external flow disturbances, which demands the close control of both the test conditions and the possible disturbance sources.

In the paper [1] the transition position on the 2D model was detected basing on the analyses of the measured integral (over the spectrum) pulsations of the longitudinal velocity component at different *X/C* and frequency spectra of the disturbances.

More strict approach to the detection of the laminar flow destruction boundary is investigation of the intermittency function in the boundary layer. To realize this approach, in the papers [2, 3] the intermittency γ was investigated as a function of the longitudinal co-

ordinate, that demanded the elaboration of the intermittency detector for the hot-wire oscillograms analyses. Main difficulty in this case is the choice of the threshold value allowing distinguish laminar and turbulent signals. As the detector functions for the high-frequency turbulent pulsations, the squared first and second time derivatives of the signal were used. The automated choice of the threshold was performed in dependence with the type of the surveyed disturbances according to the technique described in the paper [5]. Correctness of γ definition was confirmed by comparison of the obtained dependencies $\gamma(y)$ for the developed turbulent boundary layer with similar results of Blair [6].

The results of the corresponding measurements [2] demonstrated that at the natural disturbance background at X/C = 0.585 there was a boundary layer separation with the creation of separation bubble in the X/C = 0.59-0.65 zone. It was the region where laminar-turbulent transition in the flow took place.

During the tests with the turbulizing grids, the minimal value of the longitudinal co-ordinate where measurements in the boundary layer could be performed, was X/C = 0.12. At the lower X/C values the hot-wire gage could not be penetrated into the boundary layer due to the strong curvature of the model surface near the leading edge.

Distributions of the function

$$F = \sqrt{-\ln(1-\gamma)}$$

along the longitudinal co-ordinate are shown in Figure 3 coupled with the curves of increase of the integral (over the spectrum) pulsations. These data were obtained by moving the gage at a constant relative height Y/δ = 0.2 from the surface, where δ – boundary layer thickness. Because of upstream of the point X/C = 0.12 the measurements were impossible, the location of the transition beginning X_t/C was obtained by means of extrapolation of the measurements upstream using least-squares linear approximation of the function $F(X/C)$ up to the intersection with the F=0 line. It appeared that X_t/C = 0.055 for grid No.1 and 0.052 for grid No.2, i.e. in both cases the laminar-turbulent transition began in the negative pressure gradient area. The location of the laminar-turbulent transition end X_T/C was defined relying on the function F value reaching 2.14 (γ = 0.99). The obtained values of X_T/C were 0.32 for grid No.1 and 0.167 for grid No.2. So, the total length (X_T/C - X_t/C) of the laminar flow destruction zone was 0.265 for grid No.1 and 0.115 for grid No.2.

As it is shown in Figure 3b, the most detailed measurements of $\gamma(X/C)$ dependence were made in the case of the lower flow turbulence level (grid No.1). It was found that in this case the $F(X/C)$ dependence may be approximated by two lines inclined to the X/C axis at different angles – the lower one at the beginning of the measurement zone and the bigger one downstream. For the first time this effect was discovered by R. Narasimha [7] when investigating the laminar-turbulent transition in flows with alternating pressure gradient. M.F. Blair [6] obtained similar behavior of the function $F(X/C)$ in the boundary layers with constant negative pressure gradient. It the paper [7] this phenomenon was called "subtransition".

At zero angle of attack the negative pressure gradient area spreads on the model LV6 surface up to X/C = 0.15, followed by the flow zone practically without pressure gradient. It is possible to assert that the subtransition effect observed here is also associated with negative pressure gradient.

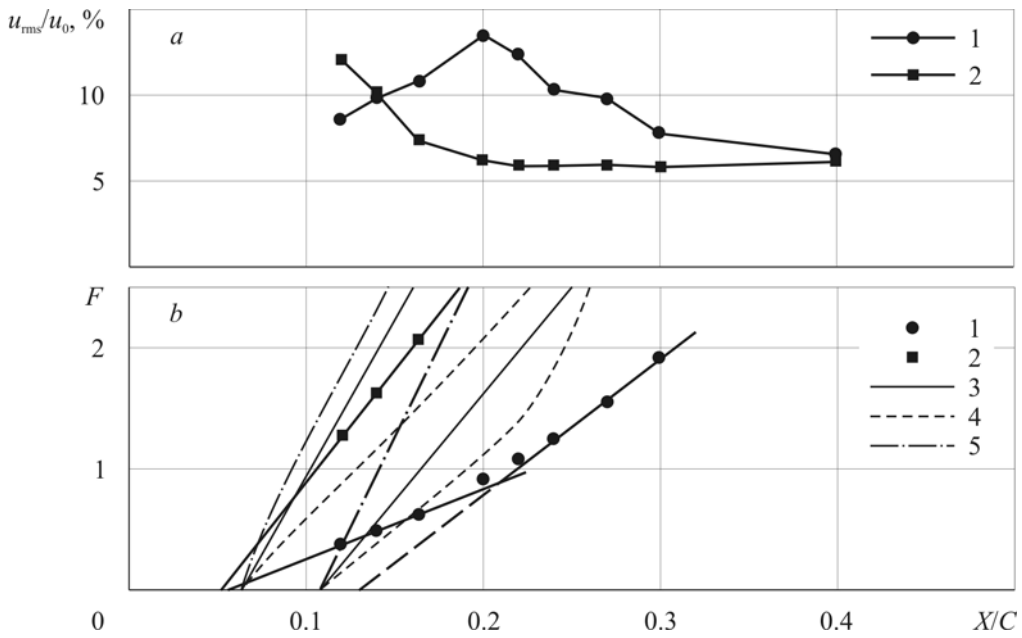

Figure 3: a) – longitudinal distribution of the integral over spectrum rms pulsations amplitude for $Y/\delta = 0.2$. b) – longitudinal distribution of the function F: 1 – grid No.1, 2 – grid No.2, 3 – intermittency function model [9], 4 – calculation using model [10], 5 – calculation using model [11]. Thick lines show linear approximations of the experimental points.

There exist two hypotheses explaining the subtransition effect. R.E. Mayle [9] proposed that generation of turbulent spots is distributed over a certain area along the longitudinal co-ordinate. Alternative hypothesis of W.J. Solomon et al. [10] conserves the assumption [8] about the fixed generation point, however it introduces the dependences of such turbulent spots characteristics as velocity and angle of their propagation, from pressure gradient. In the grid No.2 case the subtransition effect was not discovered in our experiments, what is evidently explained by the above-mentioned upstream restriction of the measurement zone.

The influence of the acoustic disturbances on the laminar-turbulent transition location was also defined from the analyses of the intermittency function distribution γ along the longitudinal co-ordinate. For sound with frequencies $f_s \geq 1600$ Hz values of X_t/C appeared to be rather close to the average for all investigated f_s values of X_t/C being equal to 0.563.

As it may be concluded from the data analyses, the acoustic disturbances of the external flow excite the unsteady Tollmien-Schlichting waves in the model boundary layer. The development of these waves up to $X/C = 0.4$ is linear (or close to linear). Value of X_t/C, obtained at the acoustic exciting of the Tollmien-Schlichting waves turned out to be not much less than boundary layer separation co-ordinate $X_s/C = 0.585$, obtained in natural conditions. Laminar-turbulent transition doesn't have time to finish before the boundary layer separation. The rms velocity pulsations at $X/C = 0.6$ also reach just relatively low values of 5-6%. It may be concluded that in the exciting frequencies f_s range from 1200 to 3000 Hz at the achieved in these experiment levels of acoustic pressure p_s of 91-108 dB the acoustic disturbances lead only to insignificant shift of the transition beginning line upstream from the separation point.

4 ANALYSIS OF THE TRANSITION PREDICTION USING DIFFERENT METHODS

4.1 Empirical and semiempirical transition criteria

Empirical and semiempirical transition models are traditionally widely used in the engineering practice. Comparison of the results obtained here with predictions basing on such models is of interest. For separation bubbles corresponding correlations are presented in [8,12]. These correlations associate the location of the character points (X_t and X_T) in the flow with the Reynolds number calculated basing on the boundary layer momentum thickness at the separation point and local velocity of the external flow. S.K. Roberts and M.I. Yaras [11] proposed a transition model for wide class of 2D flows, including the separated ones. Model [11] also connects the X_t location with the Reynolds number at the separation point, but it describes the intermittency function behavior in the transition zone.

All the models considered in the conditions of our experiment give good prediction for the transition beginning co-ordinate. Mayle model [9] for "short" separation bubbles (such as in our experiment) predicts for X_t/C the value of 0.5923, being in very good agreement with the experiment. Model [11] gives X_t/C = 0.6049. For the location of X_T/C model [9] predicts substantially understated value of 0.6021, so the turbulent spots generation rate predicted by this correlation is higher than experimental one by the order of magnitude. The Walker correlation [12], based on the speculations followed from the stability theory, predicts X_T/C = 0.6436, practically coinciding with the test data. Model [11] predicts slightly shorter length of the transition zone compared with the experiment, but, nevertheless, the agreement of the results is rather satisfactory. The calculation using model [11] gives X_T/C = 0.6435.

For flows with high degree of external turbulence, the empirical correlations are widely used which connect the turbulence spots characteristics with averaged boundary layer parameters. They allow for calculating the transition zone length with the help of the formula

$$\gamma = 1 - \exp\left[-\frac{n\sigma}{U_0}\left(X - X_t\right)^2 \right],$$

where X_t – co-ordinate of the transition area beginning, n – generation rate of turbulent spots, σ – parameter depending on the angle and velocity of the turbulent spots propagation. For the value X_t definition, empirical dependencies are also used, in particular – correlations, proposed in [13, 9, 5]. Comparison of the obtained experimental data [3] with these predictions showed that correlations [13, 5] give overstating estimations for the Reynolds number of the transition beginning calculated basing on the displacement thickness. The best estimations were given by the well-known dependence between the Reynolds number (based on the momentum thickness) and turbulence level [9]

$$\mathrm{Re}_{\delta_2 t} = 400 Tu^{-5/8}.$$

As it is shown in Figure 3b, this correlation gives satisfactory results for the X_t/C position (0.108 and 0.064 for grids No.1 and No.2 respectively), although they lay downstream from the experimental values.

The transition zone extension was calculated using models [9], [10] and [11]. The results of calculations are shown in Figure 3b. Their comparison with the test data indicates that the best results for both the transition region extension and for generation rate of turbulent spots and their propagation characteristics (these values are proportional to the inclination angles of the calculated curves in the Figure) were obtained using model [10]. The model takes into consideration the dependence of these values from pressure gradient and also predicts the subtransition effect. Correlation [9] with constant turbulence spots generation rate also gives not bad results.

It should be noted that all studied correlations give the understating extension of the transition zone.

4.2 Stability-based e^N method

For definition of the laminar-turbulent transition location in the range $0.1\% \le Tu \le 1\%$ basing on the linear theory of the hydrodynamic stability, L.M. Mack [14] proposed the following empirical relation of N-factor vs. Tu:

$$N_{tr} = -8.43 - 2.4 \ln(Tu) \qquad (1)$$

Calculated dependence of N-factor from the longitudinal co-ordinate for the present experimental conditions is shown in Figure 4. The calculation was performed on the basis of the numerical matrix method of the hydrodynamic stability analyses of three-dimensional boundary layer [15]. This correlation enabled to define the N-factor values for the character points X_t/C and X_T/C, also shown in the Figure. As it follows from Figure 4, for the cases with increased external turbulence, the N-factor values corresponding to the X_t/C position are equal to zero, i.e. in these cases transition began before the loss of stability of the boundary layer (by-pass transition).

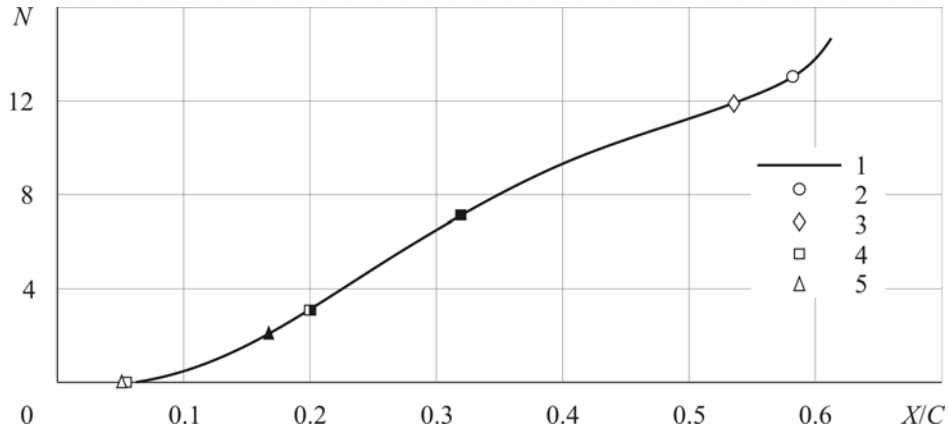

Figure 4: N-factor dependence from the longitudinal co-ordinate. 1 – calculation, 2 – natural conditions, 3 – f_s = 2.8 kHz, 4 – grid No.1, 5 – grid No.2. Open symbols show the transition beginning, filled symbols – points γ = 0.99, semi-filled – position of the longitudinal pulsations maximum for grid No.1.

In Figure 5 corresponding N-factor values are shown in comparison with the relation (1). For $Tu \le 0.1\%$ formula (1) gives understated values of the transition N-factor, because in this case the acoustic disturbances of external flow play the main role. In the case of $Tu = 0.91\%$

(grid No.2) correlation (1) predicts overstated value of the transition *N*-factor. At $Tu = 0.61\%$ formula (1) leads to satisfactory results, if value X/C corresponding to the maximum in the longitudinal distribution of flow pulsations (Figure 3a) is considered to be the transition point.

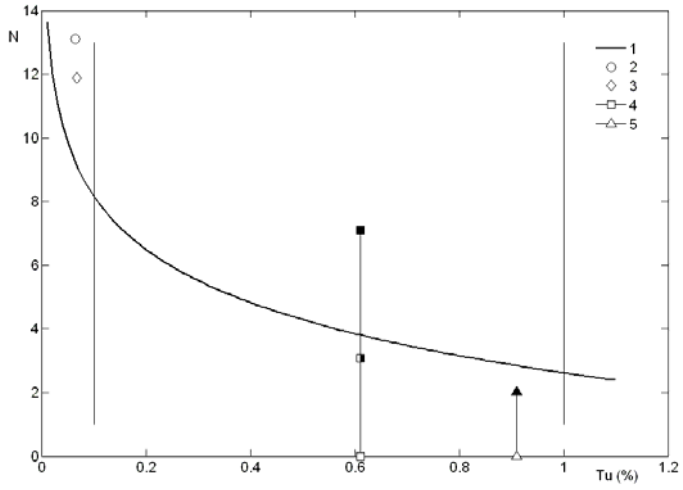

Figure 5: Dependence of the transition *N*-factor from the turbulence level: 1 – formula (1), other designations – as in Figure 4. Vertical lines show the limits of formula (1) validity.

4.3 Transport equation methods and transition-turbulence models

This section demonstrates the results of flow calculation over the airfoil LV6 model in TsAGI T-124 wind tunnel basing on the software package ANSYS CFX [16] (TsAGI license No.501024) at the described above experimental conditions. For laminar-turbulent transition prediction on the straight wing surface turbulence models of Langtry-Menter [17] and Walters-Cokljat [18] were used.

Model $\gamma - \mathrm{Re}_\theta$ [17] was developed by F. Menter and R. Langtry on the basis of the shear stress transport equation model. The model [17] enables, in principle, to calculate the laminar-turbulent transition. The transition characteristics are defined using the intermittency coefficient γ and number $\widetilde{\mathrm{Re}}_{\theta_t} = \rho\theta U/\mu$, corresponding to Reynolds number at the transition beginning, defined using the local velocity U and momentum thickness θ. Both parameters, γ and $\widetilde{\mathrm{Re}}_{\theta_t}$ are defined from the solution of the corresponding differential transport equations.

The Walters-Cokljat turbulence model [18] includes: transport equation for turbulence kinetic energy k_T, transport equation for laminar kinetic energy k_L and transport equation for turbulent pulsations frequency ω. In the formulation of the Walters-Cokljat model the transport equation for the intermittency is absent, so it is not possible to compare the considered turbulent models relying on this parameter.

Figure 6 displays experimental and calculated pressure distributions in the central section of the upper wing surface. Both turbulence models demonstrate satisfactory agreement with the test measurements [19, 20].

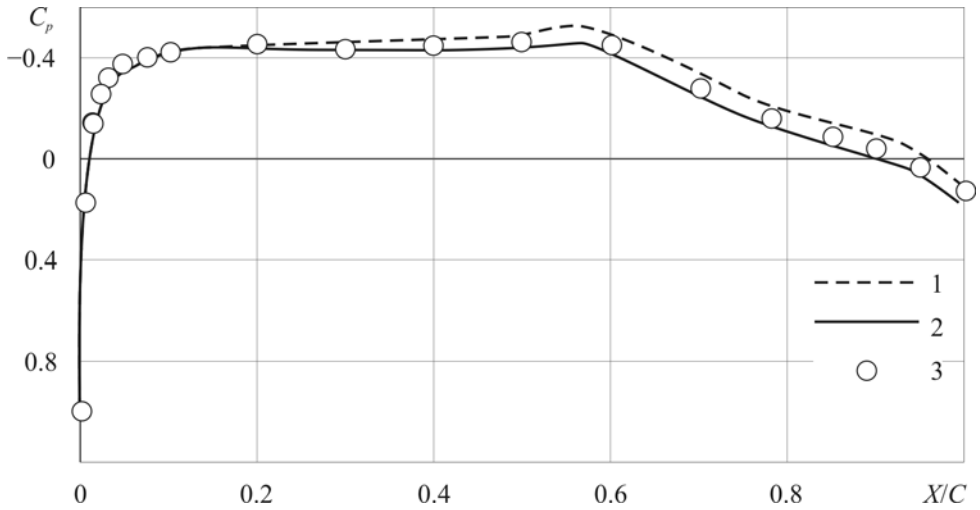

Figure 6: Pressure distribution over the upper wing surface: 1 –Walters-Cokljat turbulence model, 2 – Langtry-Menter model, 3 – experiment.

Figure 7a demonstrates experimental and predicted (Langtry-Menter model) distributions of intermittency function distribution γ in the central wing section at the natural disturbances background, and Figure 7b shows the same distributions in case of installation of turbulizing grid No.1.

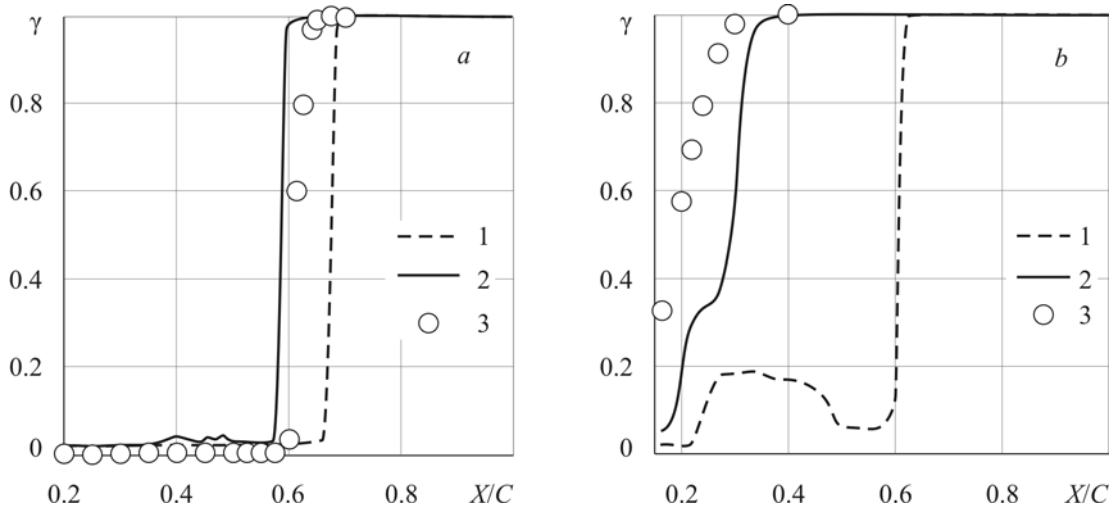

Figure 7: Distribution of the experimental and predicted (Langtry-Menter model) intermittency function γ over the upper wing surface: a) – at the natural disturbances background, b) – at the increased turbulence level of the incoming flow. 1 – prediction (wing in the WT), 2 – prediction (wing in the unbounded flow), 3 – experiment.

For modelling the turbulence grid at the entrance to the computational domain the boundary condition included turbulence intencity 0.61% and turbulent-to-molecular viscosity ratio $\mu_t / \mu = 100$. Satisfactory accuracy of the Lantry-Menter model for this type of flow may be noticed. However, our attempts to simulate the flow at higher turbulence level of the incoming flow (grid No.2) were not successfull.

5 CONCLUSIONS

- The possibilities of application of different methods for prediction of the laminar-turbulent transition and for investigation of the increased free stream disturbances effect on the transition characteristics in 2D flow are analyzed.
- All studied empirical and semiempirical transition criteria give a good prediction of the transition beginning co-ordinate, but these correlations understate the value of the transition zone extension.
- The e^N-method rather successfully correlates with laminar-turbulent transition; however, the values of N-factor corresponding to transition are substantially different for various external conditions. The empirical relation of N-factor vs. free-stream turbulence level Tu for $Tu \leq 0.1\%$ gives understated values of the transition N-factor. In the case of $Tu = 0.91\%$ this correlation predicts overstated value of the transition N-factor and leads to satisfactory results for $Tu = 0.61\%$, if the point corresponding to the maximum in the longitudinal distribution of flow pulsations is considered to be the transition point.
- The Langtry-Menter and Walters-Cokljat transition-turbulence models enables, in principle, to calculate the laminar-turbulent transition. However, additional researches are demanded to define the operational limits of the transport equation methods and transition-turbulence models to compare different models and to develop recommendations for their practical use.

REFERENCES

[1] Chernyshev, S.L., Ivanov, A.I., Kiselev, A.Ph., Kuzminsky, V.A., Sboev,D.S. and Zhigulev, S.V. Experimental and numerical investigation of the laminar-turbulent transition mechanisms in the boundary layer on 2D and 2.5D models in the low-turbulence wind tunnel. *Proceedings of 5-th European Conference on Computational Fluid Dynamics (ECCOMAS CFD 2010)*. Ed. by Pereira J.C.F., Sequeira A., Pereira J.M.C. Lisbon, Portugal, June 14–17, 2010, paper No. 1786.

[2] Vlasov, V.A., Zhigulev, S.V., Ivanov, A.I., Kiselev, A.Ph., Kuzminsky, V.A., Sboev, D.S. and Chernyshev, S.L. Laminar-turbulent transition on the LV6 laminarized airfoil: natural transition. *TsAGI Science Journal* (2011) **42**, No.5: 565-591.

[3] Vlasov, V.A., Zhigulev, S.V., Ivanov, A.I., Kiselev, A.Ph., Kuzminsky, V.A., Sboev, D.S. and Chernyshev, S.L. Laminar-turbulent transition on the LV6 laminarized airfoil. Part II: effect of free stream disturbances. *TsAGI Science Journal* (2011) **42**, No. 6: 729-756.

[4] Filippov, V.M. Characteristics of fluctuations in flow through low-turdulence arerodynamic wind tunnel T-124 designed for small speeds. *Uchenye Zapiski TsAGI.* (2008) **39**, No.1-2:68-80 (*in Russian*).

[5] Fransson, J.H.M., Matsubara, M., Alfredsson, P.H. Transition induced by free-stream turbulence. *J. Fluid mech*. (2005) **527**: 1-25.

[6] Blair, M.F. Boundary-layer transition in accelerating flows with intense freestream turbulence: Part 2 – The zone of intermittent turbulence. *J. Fluids Engineering*. (1992) **114**: 322-332.

[7] Narasimha, R. Subtransitions in the transition zone. *Laminar-Turbulent Transition*. Ed. by V.V. Kozlov. Berlin: Springer-Verlag, (1985). P. 141-151.

[8] Dhawan S., Narasimha R. Some properties of boundary layer flow during the transition from laminar to turbulent motion. *J. Fluid mech.* (1957) **3**:418-436.

[9] Mayle, R.E. The role of laminar-turbulent transition in gas turbine engines. *J. Turbomachinery*. (1991)**113**:509-537.

[10] Solomon, W.J., Walker, G.J., Gostelow, J.P. Transition length prediction for flows with rapidly changing pressure gradients.*J. Fluids Engineering*. (1996)**118**:744-751.

[11] Roberts, S.K., Yaras, M.I. Modeling transition in separated and attached boundary layers. *J. Turbomachinery*. (2005) **127**: 402-411.

[12] Walker, G.J. The role of laminar-turbulent transition in gas turbine engines: a discussion. *J. Turbomachinery*. (1993) **115**: 207-217.

[13] Abu-Ghannam, B.J., Shaw, R. Natural transition of boundary layers: the effects of turbulence, pressure gradient and flow history.*J. Mech. Eng. Sci*. (1980) **22**. No. 5:213-228.

[14] Mack, L.M. Transition prediction and linear stability theory.*AGARD CP*-224.(1977). P. 11-22.

[15] Kuzminsky, V.A. Matrix numerical method of stability calculation of three-dimensional boundary layers. *Uchenye Zapiski TsAGI*. (2007) **38**, No. 3-4:44-56 (*in Russian*).

[16] Menter, F.R., Galpin, P.F., Esch T., Kuntz M., Berner C. CFD Simulations of Aerodynamic Flows with a Pressure-Based Method. *Proceedings of 24th International Congress of the Aeronautical Sciences(ICAS 2004)*. Japan, Yokohama, 2004. 14 p.

[17] Langtry, R., Menter, F. Correlation based transition modelling for unstructured parallelized computational fluid dynamic codes. AIAA Journal. (2009) **47**. No. 12.

[18] Walters, D.K., Cokljat, D. A three-equation eddy-viscosity model for Reynolds-averaged Navier-Stokes simulations of transitional flows. *Journal of Fluids Engineering*.(2008) **130**.No.12: 14 p.

[19] Vozhdaev , V.V., Kiselev, A.Ph., Kuzminsky, V.A., Sboev, D.S., Teperin, L.L., Chernyshev, S.L. Numerical modeling of the position of a laminar-turbulent transition on a wing with the laminar airfoil LV6. *TsAGI Science Journal* (2013) **44**, No. 1: 65-76.

[20] Vozhdaev , V.V., Kiselev, A.Ph., Kuzminsky, V.A., Sboev, D.S., Teperin, L.L., Chernyshev, S.L. Comparison of the methods of calculation of laminar-turbulent transition parameter on the wing. Numerical modeling of the position of a laminar-turbulent transition on a wing with the airfoil LV6. *TrudyTsAGI* (2013) No. 2726. 25 p. (*in Russian*).